Capping Transmembrane Helices of MscL with Aromatic Residues Changes Channel Response to Membrane Stretch†

Chien-Sung Chiang,‡ Lena Shirinian,‡ and Sergei Sukharev*

Biology Department, University of Maryland, College Park, Maryland 20742

Received April 23, 2005; Revised Manuscript Received June 22, 2005

ABSTRACT: Tyrosines and tryptophans that anchor both ends of the helices to membrane interfaces in many transmembrane proteins are not common in MscL and homologous mechanosensitive channels. This characteristic absence of two aromatic "belts" may be critical for MscL function as the opening transition is predicted to be associated with a strong helical reorientation. A single tyrosine (Y75) on the extracellular side of the M2 helix of pentameric EcoMscL is absent in TbMscL, which instead has a single tyrosine (Y87) on the cytoplasmic side of M2. Moving the tyrosine of EcoMscL to the intracellular side (Y75F/F93Y) or capping the TM2 helix on both sides (F93Y/W) slows the kinetics of gating and increases the threshold for activation, leading to a partial loss-of-function in osmotic shock survival assays. Increasing the distance between the caps (L98W, L102Y/W) partially restores channel function presumably by loosening restraints for tilting. Capping the TM2 helix with a charged residue (Y75E) causes a right shift of the activation curve ("stiff" phenotype) and abolishes function. Introducing a "cap" into the TM1 helix (I41W) decreases the activation threshold and shortens the mean open time but unexpectedly leads to a complete loss-of-function in vivo. The data are consistent with the view that restraining helical positions in MscL by introducing specific protein−lipid interactions at membrane interfaces compromises MscL function. Subtle differences in osmotic shock survival are more evident at low levels of mutant protein expression. We observed a correlation between the right shift of tension activation threshold and the loss-of-function channel phenotype, with a few exceptions that point to other parameters of gating that may define the osmotic rescuing ability in vivo.

Bacterial mechanosensitive channels are uniquely suitable systems for studies of conformational rearrangements underlying gating transitions. The large conductance mechanosensitive channel from *Escherichia coli* (EcoMscL) gated directly by membrane tension has been extensively studied using molecular genetic, biochemical, and biophysical approaches (*1*−*3*). The crystal structure of the MscL homologue from *Mycobaterium tuberculosis* (TbMscL) in its closed conformation was determined to a 3.5 Å resolution (*4*), revealing a homopentameric assembly of two-transmembrane domain subunits. The TM1 helices, more hydrophilic in nature, are tightly packed in the core of the closed channel complex, whereas the largely hydrophobic TM2 helices form most of the lipid-facing boundary of the protein. To relate ample functional data collected mostly on the *E. coli* channel, a homology model of EcoMscL derived from the TbMscL crystal structure was subsequently proposed and analyzed (*5*, *6*).

The hallmark of MscL activation is its exceptionally high unitary conductance (∼3 nS in 300 mM salt) implying a large-scale conformational change. When the crystal structure, as well as the EcoMscL homology model, was used as initial conformation, several possible pathways for the opening transition were inferred (*6*). The initial hypothesis was that under membrane tension the cytoplasmic ends of TM1 domains move apart and TM2 helices wedge between TM1s forming a barrel-like aqueous pore made of almost parallel helices-staves (*4*, *7*). An alternative model of the open state suggested a concerted tilting of TM1−TM2 pairs associated with a simultaneous outward movement in an iris-like manner (*5*, *6*). The latter model received experimental support by cysteine cross-linking (*8*) and EPR experiments (*9*). The predicted tilting of TM1−TM2 helical pairs by about 35° produces a 3 nm-wide pore and leads to a substantial shortening of the channel barrel. This flattened conformation was expected to produce a thickness mismatch with the surrounding lipids, which was supported by the reduced pressure thresholds for MscL channels reconstituted in lipid bilayers made of shorter chain lipids (*10*). In addition to the thickness of the hydrocarbon layer, the chemical nature of lipid headgroups and related lateral pressure profiles in the surrounding bilayer were found to be important determinants for the energetics of gating (*11*, *12*).

Chemical heterogeneity of lipid bilayers in the transversal direction produces another level of complexity in protein−lipid interactions. Structural analysis of a large variety of

† The work was funded by the NASA NAG21590 research grant to S.S.

* Corresponding author: Sergei Sukharev, Biology Department, University of Maryland, College Park, MD 20742. Phone, 301-405-6923; fax, 301-314-9358; e-mail: sukharev@umd.edu.

‡ The first two authors contributed equally to this study.

[1] Abbreviations: MscL, mechanosensitive channel of large conductance; TM1/2, transmembrane helix 1 or 2; WT, wild-type; LB, Luria−Bertani bacterial medium; IPTG, isopropyl-β-D-thiogalactopyranoside; PVDF, polyvinylidene fluoride.

10.1021/bi050750r CCC: $30.25
Published on Web 08/26/2005

membrane proteins have indicated that aromatic residues Tyr and Trp are enriched at the ends of TM helices, having specific affinity for the polar/apolar interface of the membrane, coinciding with the region of phospholipid carbonyls and glycerols (*13*). These residues were proposed to anchor the ends of TM segments to the membrane interface and thereby stabilize the protein structure. The distribution of amino acids in the transmembrane domains and flanking regions in MscL proteins from 35 bacterial species was found to be nonrandom (*6*, *7*, *14*). Phenylalanines frequently occur in all 35 MscL homologues , preferentially in the second transmembrane domains (TM2) facing the lipid. Tyrosines or tryptophans, in contrast, occur infrequently in the helixes and never on both ends. EcoMscL and other species from the same subfamily have only one Tyr located at the periplasmic end of TM2 (Y75 of EcoMscL), while representatives of the more distant mycobacterial subfamily typically have two tyrosines, both at the cytoplasmic side of TM2 (Y87 and Y94 in TbMscL).

Here, we examine how the osmotic rescuing function in vivo and gating parameters of MscL in electrophysiological experiments depend on the presence and specific positions of aromatic anchors at the ends of transmembrane helices. We perform hypotonic shock experiments to evaluate the ability of mutants to rescue *mscL*$^-$, *mscS*$^-$ cells from osmotic lysis and compare it with wild-type MscL. In parallel, we use patch-clamp recording in giant spheroplasts to characterize the energetic and kinetic properties of the mutant channels and to correlate these parameters with the osmotic rescuing function.

MATERIALS AND METHODS

Strains and Molecular Modifications. Mutants were generated by the modified "megaprimer" technique (*15*). Two rounds of mutagenic PCR with *Pfu* DNA Polymerase (Stratagene) were performed with the wild-type *mscL* ORF (plasmid p5-2-2b (*16*)) as the template. The amplified mutant ORFs were gel-purified, digested with BglII and XhoI, and cloned into the pB10b vector, behind the p_{lacUV5} inducible promoter. This procedure was followed by automated DNA sequencing to confirm the validity of the clone. Single aromatic substitutions, I41W, Y75F, I79W, F93Y, F93W, L98W, L102W, and L102Y, two double substitutions, Y75F/F93Y and I79W/F93W, and a charge substitution, Y75E, were introduced. All constructs and WT MscL were cloned into the pB10b vector and transformed into MJF455 *mscS*$^-$, *mscL*$^-$ cells (*17*) kindly provided by Dr. Ian Booth (University of Aberdeen, U.K.) for hypo-osmotic shock experiments. For patch-clamp experiments, the mutants were expressed in PB104 ($\Delta\Omega$3a) *mscS*$^+$, *mscL*$^-$ cells (*18*), in which intact MscS could be used as an internal tension gauge.

Growth Curves and Osmotic Shock Survival Assays. Overnight cultures were adjusted to equal density with fresh LB and inoculated (1:200) in 250-mL flasks containing 40 mL of LB with 1 mM ampicillin. Growth of mutants was measured by reading OD_{600} under standard shaking conditions (37 °C, 255 rpm) every 30 min. The duplication time during early and mid-logarithmic phases and the maximum OD_{600} upon reaching the stationary phase were determined as growth parameters.

To assess the osmotic survival of mutants, overnight cultures of MJF455 cells carrying one of the expression vectors were grown in LB media in the presence of 100 μg/mL ampicillin. One milliliter of the overnight cultures was transferred into 20 mL of LB supplemented with 0.5 M NaCl (Hi LB, 910 mOsm) and grown to an OD_{650} of 0.6 for experiments without induction. In experiments with induced cultures, cells were grown to an OD_{650} of 0.3−0.4, induced with 0.8 mM IPTG, and grown further for 20−30 min to reach OD_{650} of 0.6 ($\pm$0.02). After the period of induction, or after reaching the above OD_{650}, 500 μL of each culture was transferred into a culture tube containing 5 mL of HiLB (for control) or 5 mL of LB diluted two times with deionized water (LB/2, 200 mOsm) and left at room temperature for 15 min. The cell samples were then diluted 10^3 or 10^4 times with the same shock medium (LB/2) and plated on standard LB plates in duplicates. For survival controls, the HiLB-adapted cultures were transferred into 5 mL of HiLB (no shock), diluted in HiLB, and plated on standard plates. The following day, the colonies were counted manually with both the mean and standard errors determined.

Control of Protein Expression. One-milliliter samples of induced and noninduced cultures at OD_{650} of 0.6 (6.7×10^8 cells/mL or 85 μg/mL dry weight (*19*)) prepared for osmotic survival tests were withdrawn before harvesting. Cells were French-pressed, and the membranes were collected by centrifugation at 17 000*g* for 35 min. The membrane pellet was dissolved in 50 mL of 2× SDS sample buffer and heated to 60 °C for 10 min. The volume of samples per well applied to the gel was always 20 μL for uninduced cultures and 8 μL for induced cultures. Membrane proteins were resolved on SDS gels and electroblotted on PVDF Immobilon membranes, and the MscL band was visualized with primary antibodies raised against the N-terminus (*16*) and AP-conjugated secondary antibodies. Both strips of PVDF membrane containing induced and noninduced samples were incubated with antibodies, washed, and developed with Western Blue stabilized alkaline phosphatase substrate (Promega) in the same tray under identical conditions. Digital images of membranes were taken under transillumination on an Alpha Imager (Alpha Innotech, San Leandro, CA), and the amounts of color in the bands were subjected to digital densitometry. The background color density distribution in the PVDF membrane was reconstructed based on values in protein-free areas outside the bands and subtracted from values within the bands using custom-written program GELAN (A. Anishkin).

Electrophysiological Analysis. For patch-clamp experiments, the mutants were expressed in PB104 cells. Preparation of giant spheroplasts, patch-clamping, and pressure protocols were as described previously (*20*, *21*). Intact MscS channel present in PB104 cells activated at 5.5 dyn/cm was used as an internal tension gauge to convert pressure into the scale of tension (*21*). *P*o was determined as I/I_{max}, where I_{max} was the current obtained at saturating pressure. Open dwell time histograms usually containing no less than 2000 opening events were collected at low *P*o (10^{-3}−10^{-2}) and analyzed using PClamp 9 software (Axon Instruments).

RESULTS

The Gating Model and the Choice of Positions for Substitutions. The iris-like mechanism of MscL is illustrated in Figure 1. It has been shown previously that, to satisfy the

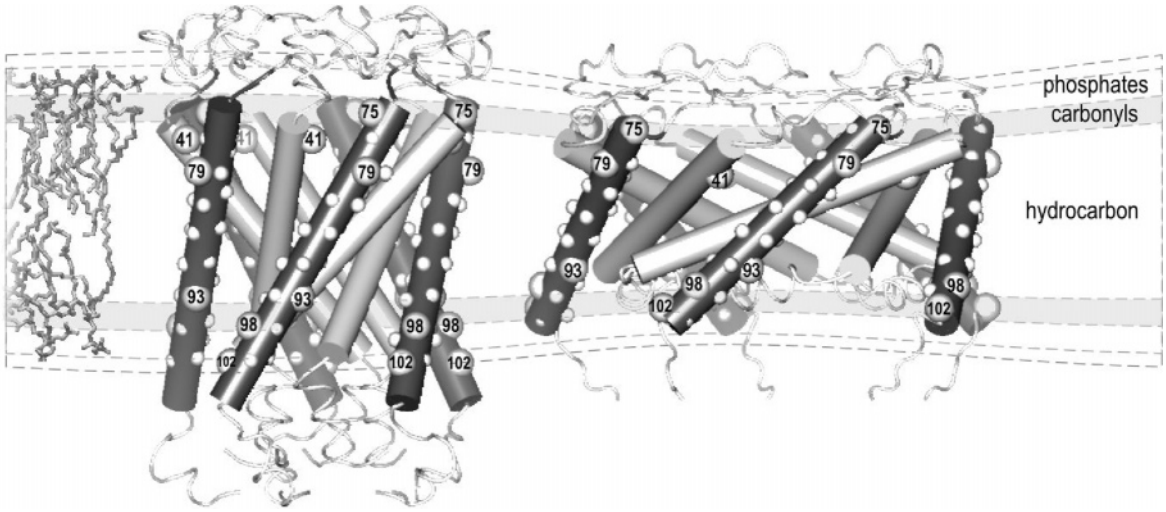

FIGURE 1: Models of the EcoMscL transmembrane barrel in the closed and open states. Opening of a 3 nm water-filled pore is associated with the increase of TM1 tilt from ~30° to ~65° relative to the membrane normal. The positions of alpha carbons on lipid-facing helices are shown as hemispheres, and the residues targeted by mutations are numbered. The models are aligned with the layered distribution of chemical groups in the simulated POPC bilayer (Feller, S., http://persweb.wabash. edu/facstaff/fellers/coordinates/popc.pdb) shown on the left. Since the open conformation of the barrel is substantially flattened, a hypothetical thinning of the bilayer around the protein can be expected. Capping of both ends of the TM2 helices with aromatic residues is predicted to restrain their ability to tilt.

measured unitary conductance, the transmembrane barrel has to expand by 20−23 nm^2 producing a water-filled pore of 3 nm in diameter (*21*). This conformation with TM1 helices tilted at 65−70° to the pore axis was previously supported by the A20C−L36C cross-link (between two adjacent TM1), also shown to stabilize the open state of the channel (*8*). Another bridge, I32C−N81C, linking TM1 and TM2 of two subunits, permitted channel gating thus suggesting that adjacent TM1 and TM2 do not change their relative positions substantially during opening and thus should tilt together (*8*). This pairing of helices predicts a strong tilt for TM2 as well, and must produce a substantial flattening of the helical scaffold of the barrel (*6*, *22*). The figure illustrates the positions of several lipid-facing residues relative to the layered distribution of chemical groups in the surrounding bilayer, upon which the models of the closed and open states are superimposed. Because the flattened open conformation is expected to distort boundary lipids, a thinning of the bilayer is expected. The figure is highly schematic and represents only the predicted spatial scale of helical rearrangements in a typical bilayer, but does not take into account the actual conformations of the boundary lipids and side chains in this highly anisotropic environment.

The scheme shows that in the tightly packed closed state, the distribution of aliphatic and aromatic residues generally corresponds to the hydrocarbon core and the adjacent layers of carbonyls/glycerols. On the outer surface, Y75 lays just at the level of carbonyls and I41 on TM1 probably faces the nearby hydrocarbon. On the inner surface, it is likely that F93 (homologous to Y87 in TbMscL) also resides at the hydrocarbon boundary or in the carbonyl/glycerol layer. L98 situates amid carbonyls and glycerols, and L102 likely extends into the level of phosphate groups, although it is hard to predict the exact conformation of its side chain. When MscL opens, TM1 helices are predicted to tilt more than TM2. We presume that in the open state Y75 stays in its most favorable environment, the carbonyl/glycerol layer, while tilting of the helices submerges their opposite (cytoplasmic) ends deeper into the hydrocarbon, posing no apparent hydrophobic conflict. Having this scheme, we hypothesize that aromatic (Y or W) substitutions for F93 or L98 at the end of TM2 stabilize more upright positions of helices (closed state) as tryptophans and especially tyrosines have higher affinities to this anisotropic boundary layer of intermediate polarity. Tilting may require either a costly repositioning of these aromatic anchors from the carbonyl-occupied zone or stronger distortion of the boundary lipids. The presence of aromatic anchors on one side, and never on both ends of the lipid-facing helices in all known MscL homologues (see alignments in refs *4*, *7*, and *14*), may serve its purpose. The experiments below are designed to answer the questions of what would happen if the aromatic anchors in EcoMscL were moved to the cytoplasmic side of TM2, as they are in mycobacterial MscLs, and what would be the effect of having aromatic anchors on both ends of the helices?

Among the mutations introduced in the lipid-facing TM2 helix, Y75F removes a canonic aromatic anchor, and Y75E replaces it with a negatively charged cap. The double Y75F/F93Y mutation moves tyrosine from the periplasmic to the cytoplasmic end of TM2. When introduced on the wild-type background, mutations F93Y, F93W, L98W, L102Y, and L102W add the second aromatic cap on the cytoplasmic side, at different distances from the existing extracellular cap (Y75). The I79W mutation adds the second anchor to the periplasmic end of TM2 one helical pitch below Y75, whereas double I79W/F93W has two aromatic residues on the periplasmic side and one on the cytoplasmic side. Additionally, the I41W mutation introducing an aromatic cap on the extracellular end of TM1 was generated.

Protein Expression and Osmotic Survival of Mutants. WT and all mutants were expressed in MJF455 (*mscL-*, *mscS-*) bacteria and tested for their rescuing ability against a 700 mM osmotic downshock. Bacteria were pregrown in the high-osmotic medium (HiLB, 900 mOsm), diluted into low-osmotic medium (LB/2, 200 mOsm), and plated after several serial dilutions. The magnitude of osmotic downshift (700 mOsm) was adjusted to inactivate 99% of the control

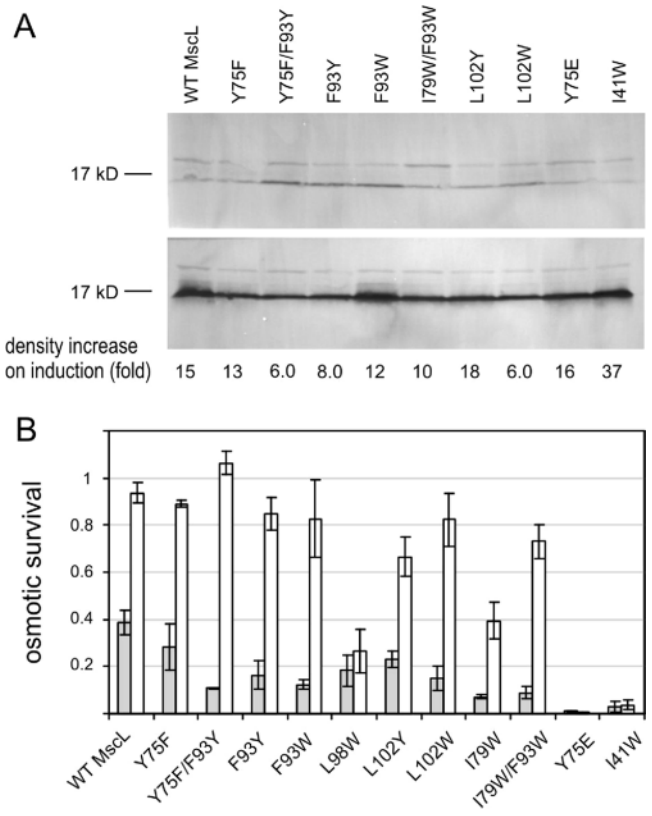

FIGURE 2: Expression levels of mutant proteins and osmotic survival of MJF455 bacteria under noninducing and inducing conditions. (A) Western blots of membrane samples developed with anti-MscL antibodies without (top) and with 25 min induction by IPTG (bottom). The fold for total density associated with the MscL band is indicated (corrected for 2.5 larger applied sample volume in uninduced preparations). Expression levels of the I79W and I79W/F93W mutants under similar conditions were examined separately and found comparable to WT (data not shown). (B) Survival of MJF455 cells expressing different MscL mutants upon a 700 mOsm osmotic downshift. Induced cultures (white bars) express more channel protein, and their survival appears to be less sensitive to mutations. The survival of severe loss-of-function mutants Y75E and I41W is low and independent of the level of expression. The survival of the empty vector control (pB10b plasmid) under both inducing and noninducing conditions was no higher than 0.5%.

MJF455 cells carrying empty vector, but to retain about 40% survival when WT MscL is expressed at a low level. High levels of WT MscL expression resulted in 95% survival. The procedure was repeated at least three times for each mutant, with both induced and noninduced cultures.

Prior to osmotic shock, 1 mL of each culture was sampled, and the MscL protein content was quantified using Western blots. As shown in Figure 2A, all mutant proteins were produced at a fairly uniform level, comparable to WT MscL. Even without induction, an appreciable amount of channel proteins is produced through the p_{lacUV5} promoter "leakage". This amount corresponds to 3−5 channels per patch sampled with standard 0.5 μm pipets (*21*). The densitometry indicated that the total amount of color associated with each protein band increases 3−14 (5.5 times in average) upon induction of the p_{lacUV} promoter with 0.8 mM IPTG. Given the difference in gel loading (2.5 times larger sample volume for noninduced samples), the total increase in protein expression level is 14-fold in average, consistent with the number of channels per patch found in induced and noninduced spheroplast preparations (see Table 1). Somewhat lower levels of the I41W protein was observed under noninducing conditions, but with induction, the density of the corresponding band was comparable to WT and other mutants.

Table 1: Growth Parameters for Mutants Displaying Pronounced Loss-of-Function Phenotypes[a]

mutant	duplication time uninduced (min)	duplication time in 1 mM IPTG (min)	OD_{600}^{max} stationary phase
WT	26.4	35.0	2.76
I41W	27.2	38.5	2.74
Y75E	27.1	37.1	2.82
L98W	26.8	36.8	2.78
F93W	27.3	35.1	2.82
I79W	27.5	35.7	2.76

[a] The duplication time for uninduced cultures was measured in the early log phase, between OD_{600} 0.01 and 0.9. To induce the cultures, IPTG was added at 90 min ($OD_{600} \sim 0.3$); thus, the values of duplication time in the middle column are given for the range of OD_{600} between 0.3 and 1.5.

Figure 2B presents cell survival upon a 700 mOsm osmotic downshock for each of the mutants and cumulative Table 2 compares survival with the electrophysiological properties of the channels. All substitutions compromise the rescuing function of MscL to a different degree. A removal of the conserved extracellular aromatic cap (characteristic for the EcoMscL subfamily) through the Y75F substitution led to insignificant differences in survival under induced conditions and only a mild decrease under low-copy expression, compared to WT. Moving the aromatic cap from the periplasmic to the cytoplasmic side (Y75F/F93Y) led to a significant decrease in survival in uninduced cultures, but essentially no change in induced cultures. Addition of the second aromatic cap at position 93 (F93Y or F93W) reduces survival only in uninduced cultures. Extending the distance between the caps along the helix in the L98W or L102Y/W mutants shows tendencies to improve survival under low-copy conditions, but for some reason, this did not correlate with the survival under full induction for L98W. The second aromatic cap at the periplasmic side (I79W) or in combination with a cytoplasmic cap (I79W/F93W) strongly compromises channel performance under noninduced conditions. Y75E or I41W result in a complete loss of function, in both uninduced and induced cultures. On the basis of the densities of bands on the Western blot (panel A), this drastic decrease of viability cannot be explained by low expression of these proteins; however, the number of active channels per patch (see Table 2 and below) was considerably lower in I41W spheroplast preparations than in WT. The magnitudes of changes illustrate that low-copy expression conditions better resolve subtle differences between the mutants. Performing survival tests with full induction masks subtle differences in mild mutants, but confidently reveals severe loss-of-function phenotypes.

To ensure that the low osmotic survival of the mutants is not a result of toxic gain-of-function phenotypes (*23*), we measured growth parameters for the most compromised, I41W, Y75E, I79W, L98W, and F93W, mutants. Table 1 shows that the duplication time of all mutants in uninduced and induced cultures is indistinguishable from that of WT

Table 2: Electrophysiological Properties of Mutants and Osmotic Survival in Comparison with WT MscL[a]

		open dwell time (ms)				relative survival upon osmotic downshock	
MscL mutant	number of channels per patch, uninduced/induced	$\tau 1$	$\tau 2$	$\tau 3$	activation midpoint, $\gamma_{1/2}$ (dyn/cm)	uninduced	induced
WT	5/50	0.1	6.2 ± 2	21 ± 4	10.2 ± 0.6	1.00 ± 0.14	1.00 ± 0.1
Y75F	6/45	1.7	12 ± 2*	24 ± 4	10.3 ± 1.1	0.73 ± 0.26	0.95 ± 0.05
Y75F/F93Y	4/60	1.5	28.3 ± 2*	213 ± 14*	13.5 ± 0.6**	0.28 ± 0.01**	1.1 ± 0.05*
F93Y	6/60	0.3	25 ± 10*	80 ± 22*	13.0 ± 0.7**	0.42 ± 0.20**	0.91 ± 0.1
F93W	5/60	0.2	29 ± 17	360 ± 24*	13.2 ± 0.8**	0.32 ± 0.05**	0.88 ± 0.2
L98W	na/55[b]	<0.1	7.2 ± 4	26 ± 6	13.2 ± 0.3**	0.47 ± 0.17*	0.28 ± 0.1**
L102Y	6/70	0.8	35 ± 16*	91 ± 23*	11.6 ± 0.6*	0.60 ± 0.09**	0.71 ± 0.1
L102W	5/60	2.3	28.0 ± 20	90 ± 2*	11.5 ± 0.9*	0.4 ± 0.13**	0.88 ± 0.12*
I79W	4/50	<0.1	1.3 ± 0.1*	8 ± 2*	11.2 ± 0.5*	0.18 ± 0.02**	0.42 ± 0.1**
Y75E	na/32[b]	0.7	30 ± 12*	190 ± 50*	11.4 ± 0.9*	0.02 ± 0.01**	0.04 ± 0.01**
I41W	na/10[b]	0.6	2.2 ± 0.4*	7.0 ± 3*	8.4 ± 0.7**	0.08 ± 0.06**	0.04 ± 0.01**
pB10b	na[b]	na[b]	na[b]	na[b]	na[b]	0.005 ± 0.001	0.001 ± 0.001

[a] The percentage of cell survival for each mutant is normalized to the survival of WT under identical conditions. Asterisks show the results of paired *t*-test performed against the WT. For dwell times, $P < 0.05$ (*); for the midpoint tension ($\gamma_{1/2}$) values, $P < 0.05$ (*) and $P < 0.001$ (**), and for the relative survival *P* values, $P < 0.01$ (*) and $P < 0.001$ (**). All data are shown as mean ± standard deviation except for the survival data presented as the mean ± standard error. Number of channels per patch was averaged for 3−4 patches; standard deviation was always within 20% of the mean. [b] Not available (na).

MscL. The maximum OD_{600} reflecting the density of stationary cultures was no different, indicating that none of the mutant proteins stresses the host bacterium. No growth retardation typical of "gain-of-function" mutants (*15*, *24*) was observed on IPTG plates or in liquid cultures grown in HiLB.

Channel Gating Parameters. All studied mutants formed channels that could be activated with suction under standard patch-clamp conditions. The measurements were performed uniformly in giant spheroplast preparations, both induced and noninduced, and the cumulative data are presented in Table 2. Segments of traces illustrating typical gating patterns are shown in Figure 3, whereas the dose−response (activation) curves and kinetic characteristics of mutants most drastically deviating from WT are illustrated in Figure 4. To illustrate the correlation between relative changes in rescuing channel ability with changes in gating parameters, the osmotic survival is plotted against the activating tension ($\gamma_{1/2}$) and the predominant open dwell time in Figure 5. Consistent with the survival data, Y75F showed no strong deviation from WT either in mean open time or in activation midpoint. The double Y75F/F93Y mutants produced extremely long openings and a right shift of the activation curve, with the midpoint tension increased by 3 dyn/cm (~30%). The F93Y substitution by itself also increases open dwell time, but less than the double mutant, although the right shifts of activation in both mutants are comparable, which correlates with the reduction in shock survival. F93W is also "stiff" and sets the record for the mean open time duration, which is prolonged to about 0.4 s, that is, about 20 times the WT at a comparable *P*o near 10^{-2} (Figure 3). The dose−response curves for F93W, F93Y, and I41W and dwell time distributions are compared with WT in Figure 4. L98W, placing a tryptophan about one helical turn below F93, exhibits the same 30% shift in activating tension but, in contrast to substitutions at position 93, has an open dwell time very close to that of WT. These differences to substitutions in position 93 may be caused by different axial and angular positions of the residue in the helix. The Y or W substitutions at position L102, both exhibited slightly longer open dwell

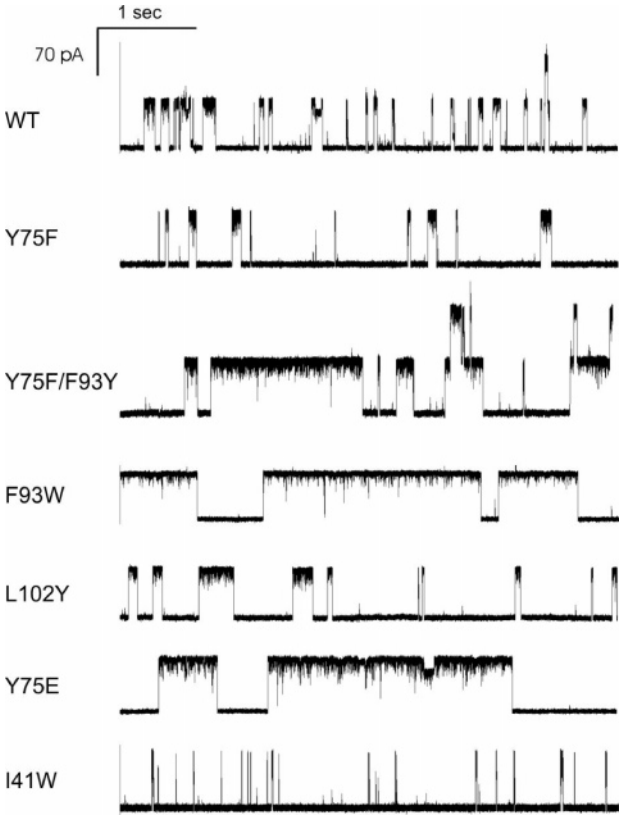

FIGURE 3: Characteristic fragments of single-channel traces recorded from giant spheroplasts expressing mutant MscLs on the *mscL*-null background (strain PB104). Currents were measured from excised inside-out patches at −20 mV under symmetrical electrolyte conditions (200 mM KCl, 10 mM $CaCl_2$, 90 mM $MgCl_2$, and 5 mM Hepes-KOH, pH 6.0). The magnitude of pressure gradients (200−300 mmHg) was chosen such that predominantly one channel was active at a time, out of 20−50 channels present in the patch, being open at *P*o between 10^{-4} to 10^{-2} (induced spheroplasts).

times and slightly higher activating pressures, but were essentially indistinguishable. Introduction of the second aromatic residue at the periplasmic end (I79W) caused a slight right shift of activation, but reduced the mean open

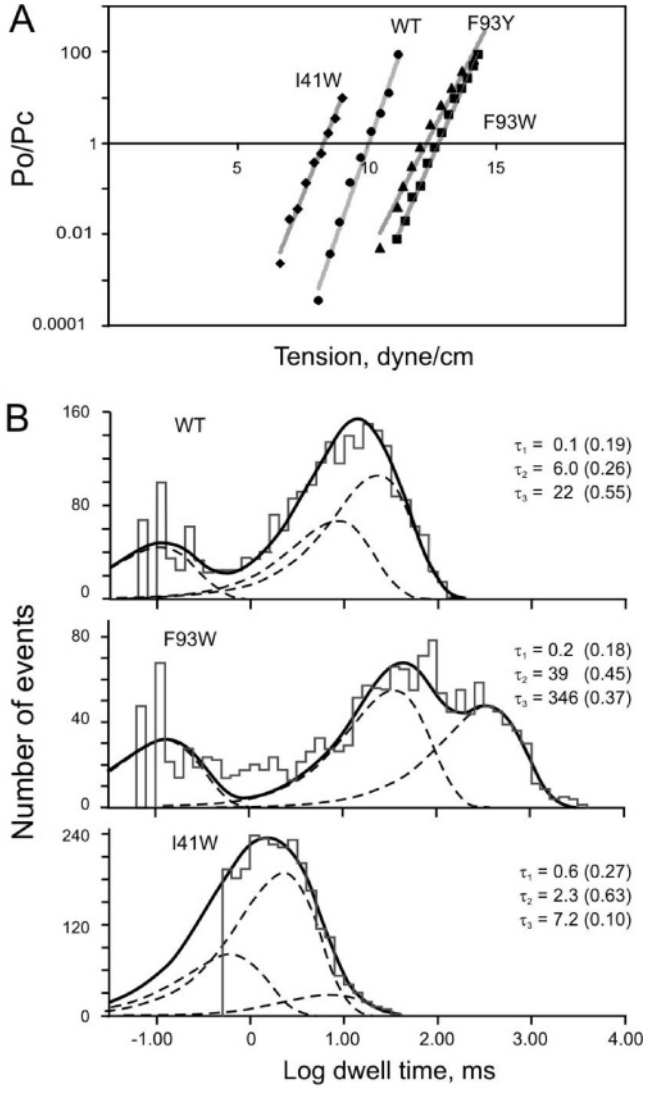

FIGURE 4: Single-channel characteristics of selected mutants which deviate drastically from WT. (A) Representative activation curves for WT, I41W, F93Y, and F93W MscL plotted as log(*P*o/*P*c) versus membrane tension. The conversion of pressure to tension scale was achieved by using the MscS activation midpoint as a reference point ($\gamma_{1/2}^{MscS} = 5.5$ dyn/cm) (*20*). All curves were fit with a two-state Boltzmann model. The ratio of open and closed probabilities *P*o/*P*c = exp[−(Δ*E* − γΔ*A*)/*kT*], where Δ*E* is the energy of the opening transition in an unperturbed membrane, Δ*A* is the protein in-plane area change (20.1 nm^2, see ref *21*), and γ is membrane tension. The midpoint, $\gamma_{1/2}$, is the intercept with the horizontal axis, where *P*o = *P*c, and correspondingly, the energy can be related to the midpoint tension as $\Delta E = \gamma_{1/2}\Delta A$. The midpoint tension shows a leftward shift in I41W while displaying a rightward shift in F93W and F93Y reflecting proportional change in energy. (B) Open time distributions for WT, F93W, and I41W MscLs fitted with three exponents. The characteristic times are denoted as τ_1, τ_2, and τ_3 with relative contributions in parentheses. The traces were recorded at P_o between 10^{-3} and 10^{-2}. Note that F93W exhibits longer open times, while I41W significantly shorter open times than WT. The cumulative data for all mutants is presented in Table 2.

time and osmotic survival. The charged cap Y75E introduced instead of the aromatic cap made the channel "stiffer" and extended the mean open time dramatically. Introduction of an aromatic cap in TM1 (I41W) markedly decreased the tension midpoint and open dwell time. The two latter mutations, as shown above (compare Figures 2B and 5), completely suppress the rescuing ability of MscL in vivo independently of the level of protein expression; however,

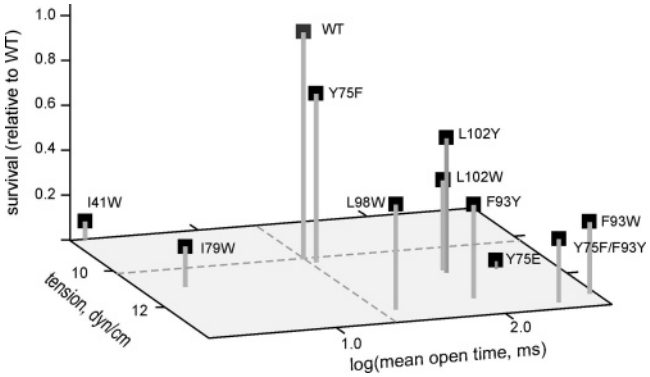

FIGURE 5: Survival of mutants under low-copy (uninduced) conditions plotted as a function of gating parameters, midpoint tension ($\gamma_{1/2}$), and mean open time. For mutants with drastically different kinetics (such as I41W, F93W) the most represented dwell times were taken in consideration. It is evident that deviation in any direction from WT parameters (indicated on the tension-dwell time plane by dashed lines) compromises the rescuing ability of the channel.

a lower number of active channels in I41W preparations (Table 2) suggests that this mutant produces unstable complexes.

DISCUSSION

Tension is transmitted to MscL through the lipid bilayer, thus, making protein−lipid interactions critical for channel function. Previous studies indicated that the lipid chain length, an asymmetrically imposed positive curvature stress (*10*), or the headgroup composition (*11*) drastically affect tension thresholds for MscL activation. Conversely, hydrophilic substitutions on the lipid-facing surfaces of MscL perturb protein−lipid interactions and reduce the channel sensitivity to tension, leading to loss-of-function phenotypes (*25*, *26*). The data presented above shows that even more subtle alterations in the lipid-facing surface of MscL via repositioning of aromatic residues can also change the gating energetics. Tyrosines and especially tryptophans are known to interact more specifically with the layer of carbonyls/glycerols than the less polar phenylalanines. TbMscL, when expressed in *E. coli*, displays an extremely "stiff" phenotype and fails to rescue cells from osmotic shock (*27*); thus, the evolutionary conservancy of different tyrosine positions in the EcoMscL and TbMscL subfamilies is mysterious and needs to be explained. It is possible that the anchoring of the protein to the lipid bilayer in the two divergent groups of bacteria was optimized to the specific lipid composition and/or character of membrane asymmetry. The two channel proteins and the corresponding lipid environments likely underwent mutual evolution and became functionally incompatible across the distant groups of microorganisms.

Tyrosine 75 is highly conserved in the EcoMscL subfamily of MscL channels (see alignments in refs *7*, *14*), but its substitution by phenylalanine does not exert strong detrimental effects on channel function either in vivo or in patch-clamp assays. It cannot be excluded that this anchor increases only the fidelity of folding or assembly, but this conjecture has yet to be confirmed. Moving this tyrosine to position 93, analogous to Y87 of TbMscL (*4*) by the double Y75F/F93Y mutation produces a pronounced decrease in cell viability upon osmotic shock, which is correlated with a

rightward shift of the activation curve by about 3 dyn/cm. This amount of shift should be considered large because the midpoint of 10 dyn/cm for WT MscL is already close to the lytic limit of the lipid bilayer (*28*) and further increases in activating tension must compromise the mechanical stability of the membrane as well as the survival. Introducing the second tyrosine, Y93, in addition to the existing Y75, produced a similar right shift.

When two aromatic caps are present at positions 75 and 93, their residence in the carbonyl-populated layers in the opposite leaflets requires the TM2 helices to be in a relatively upright position (Figure 1). Tilting may retrieve one of the anchors from its favorable environment. Extending the distance between the periplasmic and cytoplasmic aromatic caps is expected to reduce the energetic cost of tilting. Indeed, moving the periplasmic cap to positions 98 or 102 partially restores the rescuing function of MscL. Peculiarly, the introduction of the second aromatic cap to the periplasmic side (I79W), although does not shift the activation midpoint as significantly, shortens the mean open time and severely compromises the osmotic function in vivo (Figures 2 and 5).

Introduction of negatively charged glutamate in place of the single aromatic cap in the TM2 helix (Y75E) prolongs the openings, only slightly increases the activation midpoint, and completely abolishes channel function in vivo, even with maximal protein expression (Figure 2). Indeed, the right shift of activation in Y75E is less than in F93Y (based on four independent measurements, $p < 0.05$), but the detrimental effect on osmotic cell survival is more dramatic. An aromatic cap introduced on the periplasmic side of the M1 helix (I41W) reduces the activation midpoint, making the channel more sensitive to tension, and shortens the mean open time but conspicuously leads to a complete loss of function in vivo. Note that there is a disparity between the total amount of I41W protein, which is comparable to WT under inducing conditions, and the number of active channels per patch, which is five times less than in WT spheroplasts. This is suggestive of a defect in assembly or lower complex stability of this particularly mutant. Previously, the amount of left shift in activation curves was shown to be correlated with toxic gain-of-function phenotypes (*15*, *24*). Although the severity of loss-of-function phenotypes generally correlates with a right shift of activation (Figure 5), the behavior of Y75E, I79W, and I41W shows that this correspondence does not always hold true. The osmotic phenotype of I41W was conspicuous because an increase in tension sensitivity was accompanied by a complete loss of function in vivo. Previously, Levin and Blount (*23*) have shown that MscL mutants V21C, V33C, and V37C do not rescue MJF455 cells from osmotic shock. At the same time, full expression of these proteins led to a reduction of cell density at the stationary phase by more than 50%, signifying toxicity. In other words, hyperactivity (or leakiness) of these channels adversely interfered with the normal rescuing function (*15*). To test the possibility that the compromised osmotic rescuing function of some of our mutants is due to toxic (gain-of-function) phenotypes, we measured growth kinetics and the cell density at the stationary phase. As presented in Table 1, growth parameters for five mutants, including the most severe I41W and Y75E, are indistinguishable from that of WT. This excludes the plain toxic effect of these mutations leading us to conclude that, besides obvious factors such as stability of channel complexes and activating tension, other parameters such as the mean open time or preferential substate occupancy may be essential for the function of MscL in vivo. The involvement of gating kinetics was suggested by the previous study by Levin (*23*), where most of the loss-of-function cysteine substitutions in TM2, including F93C, were characterized by very short open dwell times.

Can a change in activation tension or kinetics be related to the properties of aromatic residues? Partitioning of tryptophan analogues, 3-methylindole and indole, between water and hydrocarbon or water and membrane indicated a stronger preference for membrane interface with a free-energy difference of about -3 kcal/mol relative to cyclohexane, mostly enthalpic (*29*). Thus, the energy of transfer of five lipid-facing tryptophan side chains (one per subunit) from the interfacial layer into the hydrocarbon core can be roughly estimated as 15 kcal/mol (25 kT) at room temperature. To compare this energy difference to that of phenylalanine, we can use another dataset from peptide partitioning measurements in water/octanol (mimicking hydrocarbon) and water/membrane systems affected by different "guest" residues (*13*). In these experiments W was found to be generally more hydrophobic than Y and F, with a slight preference for hydrocarbon as opposed to the interface ($\Delta\Delta G = -0.24$ kcal/mol). F exhibits a stronger preference for hydrocarbon ($\Delta\Delta G = -0.58$ kcal/mol). Y, the least hydrophobic of the three residues, prefers the interface as opposed to hydrocarbon ($\Delta\Delta G = +0.23$ kcal/mol). If we assume that gating is accompanied by a transfer of five such residues (one per subunit) from the interfacial carbonyl layer to the hydrocarbon core of the membrane, then Y and W substitutions should have effects of different magnitudes. On the basis of the $\Delta\Delta G$'s, a replacement of F93 by Y should disfavor the open state by 4 kcal/mol (about 7 kT) for a pentamer. By the same inference, W at position 93 should exert an effect of only about 1.8 kcal/mol. Our experimental observations, however, suggest that apparent changes in gating energy are larger and very similar for W and Y substitutions. The shift of the tension midpoint, $\gamma_{1/2}$, reflects a proportional increase in the apparent energy of the opening transition (Figure 4 and the legend). Given that the entire opening transition for WT MscL, which is accompanied by $\sim$20 nm^2 in-plane expansion (at $\gamma_{1/2} = 10.2$ dyn/cm), costs about 30 kcal/mol (50 kT), the substitutions that increase the $\gamma_{1/2}$ by 3 dyn/cm effectively destabilize the open state relative to the closed state by 9 kcal/mol. The Y and W substitutions at position 93 increase the gating energy by 8.7 and 8.1 kcal/mol, respectively; they also prolong the mean open time by about 1 order of magnitude, which is equivalent to the increase of the barrier for closing (i.e., energy of the transition state relative to the open state) by 1.7 kcal/mol. Thus, the picture appears to be more complex than peptide partitioning predicts. Part of the problem may stem from a highly anisotropic environment restraining the side-chain conformations in the membrane, as compared to the bulk solvent, where the side chains are expected to be free.

Although we attempted to interpret the energetic effects of substitutions in terms of penalties associated with the transfer of a particular residue from the interfacial layer to the less polar hydrocarbon, other explanations should be

considered. Flattening of the channel complex may cause a costly distortion of boundary lipids around the channel, and the coupling of the channel conformational change to the bilayer deformations may depend on the presence of aromatic anchors. Extensive studies of model peptides WALP and KALP in membranes of different thickness by Killian and co-workers (*30*−*32*) have demonstrated that tryptophans are powerful end-helix anchors which drive mutual adaptations of lipids and possibly peptides to prevent displacements of these residues from the interface. As evident from Figure 5, tryptophan substitutions are generally more deleterious for osmotic viability than tyrosine substitutions. The increased distance between aromatic caps (L98W and L102W mutations) only partially restores rescuing ability and is highly consistent with the fact that strong tilting of long Trp-capped model α-helices (WALP 23) even in thin bilayers does not occur spontaneously. In the presence of Trp anchors, tilting appears to be more unfavorable than exposure to hydrophobic surfaces (hydrophobic mismatch) (*31*) apparently because the former causes costly distortions of the more rigid interfacial layer of the membrane.

The large apparent changes in the free energy of opening caused by aromatic substitutions (8−9 kcal/mol) may reflect not only the actual change in the energy of transition but also the way the external force is applied to the protein and transmitted from the lipid bilayer to the channel gate. Indeed, these mutations may change the character of protein−lipid interactions and the pressure/tension distribution at the protein−lipid boundary. It has been suggested by several computational studies that the density of nonbonded interactions is highest in the polar layers of the membrane (*12*, *33*), and thus, tension in the bilayer must be transmitted specifically through these peripheral regions. The altered distribution of forces at the protein−lipid boundary may drive the opening transition through a different (nonoptimal) pathway, requiring a higher effective tension.

In conclusion, we have studied the effects of aromatic caps in MscL transmembrane helices on osmotic valve function and correlated the channel performance in vivo with its biophysical properties. The analysis of osmotic survival at low expression levels revealed not only strong but also subtle differences between the mutants. Controls for growth parameters ruled out toxic effects of mutations on osmotic survival. We found that the in vivo osmotic rescuing ability of MscL is clearly diminished by aromatic substitutions perturbing protein−lipid interactions at the ends of transmembrane helices. These mutations do not change the overall hydrophobicity of the protein−lipid interface but likely perturb more subtle interactions arising from specific affinities of tyrosines and tryptophans to the interfacial regions of the lipid bilayer. It appears that the structure of the lipid-facing surfaces in mechanosensitive channels is finely tuned to the specific lipid environment. Electrophysiological characterization of these mutants not only shows a general correspondence between the right shifts of activation curves and the reduction of osmotic rescuing efficiency but also indicates exceptions with no strict correlation between the two parameters. These exceptions suggest that factors other than activating tension contribute to the osmotic valve function of MscL.

ACKNOWLEDGMENT

We thank Andriy Anishkin for help in densitometric gel image analyses and for stimulating discussions. We also thank Ian Booth (University of Aberdeen, U.K.) and Paul Blount (University of Texas, TX) for the MJF455 and PB104 strains used in this work.

REFERENCES

1. Blount, P., and Moe, P. C. (1999) Bacterial mechanosensitive channels: integrating physiology, structure and function, *Trends Microbiol. 7*, 420−424.
2. Perozo, E., and Rees, D. C. (2003) Structure and mechanism in prokaryotic mechanosensitive channels, *Curr. Opin. Struct. Biol. 13*, 432−442.
3. Sukharev, S., and Anishkin, A. (2004) Mechanosensitive channels: what can we learn from 'simple' model systems?, *Trends Neurosci. 27*, 345−351.
4. Chang, G., Spencer, R. H., Lee, A. T., Barclay, M. T., and Rees, D. C. (1998) Structure of the MscL homolog from *Mycobacterium tuberculosis*: a gated mechanosensitive ion channel, *Science 282*, 2220−2226.
5. Sukharev, S., Betanzos, M., Chiang, C. S., and Guy, H. R. (2001) The gating mechanism of the large mechanosensitive channel MscL, *Nature 409*, 720−724.
6. Sukharev, S., Durell, S. R., and Guy, H. R. (2001) Structural models of the mscl gating mechanism, *Biophys. J. 81*, 917−936.
7. Spencer, R. H., Chang, G., and Rees, D. C. (1999) 'Feeling the pressure': structural insights into a gated mechanosensitive channel (see comments) (published erratum appears in (1999) *Curr. Opin. Struct. Biol. 9* (5), 650−651), *Curr. Opin. Struct. Biol. 9*, 448−454.
8. Betanzos, M., Chiang, C. S., Guy, H. R., and Sukharev, S. (2002) A large iris-like expansion of a mechanosensitive channel protein induced by membrane tension, *Nat. Struct. Biol. 9*, 704−710.
9. Perozo, E., Cortes, D. M., Sompornpisut, P., Kloda, A., and Martinac, B. (2002) Open channel structure of MscL and the gating mechanism of mechanosensitive channels, *Nature 418*, 942−948.
10. Perozo, E., Kloda, A., Cortes, D. M., and Martinac, B. (2002) Physical principles underlying the transduction of bilayer deformation forces during mechanosensitive channel gating, *Nat. Struct. Biol. 9*, 696−703.
11. Moe, P., and Blount, P. (2002) A novel approach for probing protein−lipid interactions of MscL, a membrane-tension-gated-channel, in *Biophysical Chemistry; Membranes and Proteins* (Templer, R. and Leatherbarrow, R., Eds.) pp 199−207, Royal Society of Chemistry, Cambridge, U.K.
12. Gullingsrud, J., and Schulten, K. (2004) Lipid bilayer pressure profiles and mechanosensitive channel gating, *Biophys. J. 86*, 3496−3509.
13. White, S. H., and Wimley, W. C. (1999) Membrane protein folding and stability: physical principles, *Annu. Rev. Biophys. Biomol. Struct. 28*, 319−365.
14. Maurer, J. A., Elmore, D. E., Lester, H. A., and Dougherty, D. A. (2000) Comparing and contrasting *Escherichia coli* and *Mycobacterium tuberculosis* mechanosensitive channels (MscL). New gain of function mutations in the loop region, *J. Biol. Chem. 275*, 22238−22244.
15. Yoshimura, K., Batiza, A., Schroeder, M., Blount, P., and Kung, C. (1999) Hydrophilicity of a single residue within MscL correlates with increased channel mechanosensitivity, *Biophys. J. 77*, 1960−1972.
16. Blount, P., Sukharev, S. I., Moe, P. C., Schroeder, M. J., Guy, H. R., and Kung, C. (1996) Membrane topology and multimeric structure of a mechanosensitive channel protein of *Escherichia coli*, *EMBO J. 15*, 4798−4805.
17. Levina, N., Totemeyer, S., Stokes, N. R., Louis, P., Jones, M. A., and Booth, I. R. (1999) Protection of *Escherichia coli* cells against extreme turgor by activation of MscS and MscL mechanosensitive channels: identification of genes required for MscS activity, *EMBO J. 18*, 1730−1737.
18. Blount, P., Sukharev, S. I., Schroeder, M. J., Nagle, S. K., and Kung, C. (1996) Single residue substitutions that change the gating properties of a mechanosensitive channel in *Escherichia coli*, *Proc. Natl. Acad. Sci. U.S.A. 93*, 11652−11657.

19. Gerhardt, P., Murray, R. G. E., Wood, W. A., and Krieg, N. R., Eds. (1994) *Methods for General and Molecular Bacteriology*, ASM Press, Washington, DC.
20. Anishkin, A., Chiang, C. S., and Sukharev, S. (2005) Gain-of-function mutations reveal expanded intermediate states and a sequential action of two gates in MscL, *J. Gen. Physiol. 125*, 155−170.
21. Chiang, C. S., Anishkin, A., and Sukharev, S. (2004) Gating of the large mechanosensitive channel in situ: estimation of the spatial scale of the transition from channel population responses, *Biophys. J. 86*, 2846−2861.
22. Spencer, R. H., and Rees, D. C. (2002) The alpha-helix and the organization and gating of channels, *Annu. Rev. Biophys. Biomol. Struct. 31*, 207−233.
23. Levin, G., and Blount, P. (2004) Cysteine scanning of MscL transmembrane domains reveals residues critical for mechanosensitive channel gating, *Biophys. J. 86*, 2862−2870.
24. Ou, X., Blount, P., Hoffman, R. J., and Kung, C. (1998) One face of a transmembrane helix is crucial in mechanosensitive channel gating, *Proc. Natl. Acad. Sci. U.S.A. 95*, 11471−11475.
25. Maurer, J. A., and Dougherty, D. A. (2003) Generation and evaluation of a large mutational library from the *Escherichia coli* mechanosensitive channel of large conductance, MscL: implications for channel gating and evolutionary design, *J. Biol. Chem. 278*, 21076−21082.
26. Yoshimura, K., Nomura, T., and Sokabe, M. (2004) Loss-of-function mutations at the rim of the funnel of mechanosensitive channel MscL, *Biophys. J. 86*, 2113−2120.
27. Moe, P. C., Levin, G., and Blount, P. (2000) Correlating a protein structure with function of a bacterial mechanosensitive channel, *J. Biol. Chem. 275*, 31121−31127.
28. Olbrich, K., Rawicz, W., Needham, D., and Evans, E. (2000) Water permeability and mechanical strength of polyunsaturated lipid bilayers, *Biophys. J. 79*, 321−327.
29. Yau, W. M., Wimley, W. C., Gawrisch, K., and White, S. H. (1998) The preference of tryptophan for membrane interfaces, *Biochemistry 37*, 14713−14718.
30. de Planque, M. R., Bonev, B. B., Demmers, J. A., Greathouse, D. V., Koeppe, R. E., Separovic, F., Watts, A., and Killian, J. A. (2003) Interfacial anchor properties of tryptophan residues in transmembrane peptides can dominate over hydrophobic matching effects in peptide-lipid interactions, *Biochemistry 42*, 5341−5348.
31. Ozdirekcan, S., Rijkers, D. T., Liskamp, R. M., and Killian, J. A. (2005) Influence of flanking residues on tilt and rotation angles of transmembrane peptides in lipid bilayers. A solid-state 2H NMR study, *Biochemistry 44*, 1004−1012.
32. Strandberg, E., Ozdirekcan, S., Rijkers, D. T., van der Wel, P. C., Koeppe, R. E., Liskamp, R. M., and Killian, J. A. (2004) Tilt angles of transmembrane model peptides in oriented and non-oriented lipid bilayers as determined by 2H solid-state NMR, *Biophys. J. 86*, 3709−3721.
33. Lindahl, E., and Edholm, O. (2000) Spatial and energetic-entropic decomposition of surface tension in lipid bilayers from molecular dynamics simulations, *J. Chem. Phys. 113*, 3882−3893.

BI050750R